УДК 551.46

© *Л. С. Долин*[1], *И. М. Левин*[2]
[1]Институт прикладной физики РАН, Н. Новгород
[2]Санкт-Петербургский филиал Института океанологии им. П. П. Ширшова РАН
Lev.Dolin@hydro.appl.sci-nnov.ru

ТЕОРИЯ ПОДВОДНОЙ ВИДИМОСТИ

Представлен обзор работ по теории подводной видимости. Изложена история исследований по этой проблеме. Универсальная теория подводной видимости предназначена для определения характеристик изображения и максимальной дальности видения протяженного объекта с неоднородным коэффициентом отражения для различных подводных систем видения, включая лазерные. Рассмотрены основные элементы этой теории: уравнение переноса изображения, функция размытия пучка и частотно-контрастная характеристика, алгоритмы вычисления параметров изображения объекта конечного размера, максимальная дальность видимости в воде. Параметры подводного светового поля, необходимые для этих алгоритмов, получаются в результате решения уравнения переноса излучения с использованием первичных гидрооптических характеристик. Представлена универсальная модель первичных гидрооптических характеристик для длин волн, близких к 550 нм, которая позволяет определить все используемые в теории подводной видимости первичные гидрооптические характеристики по значению показателя ослабления или даже по глубине видимости диска Секки. Описан алгоритм вычисления отношения сигнал/шум и максимальной дальности видимости в воде, который может быть использован для сравнения эффективности систем видения различных типов. Рассмотрены основные направления развития исследований подводной видимости, в частности, проблема наблюдения через взволнованную поверхность.

Ключевые слова: подводное видение, уравнение переноса изображения, функция размытия пучка, частотно-контрастная характеристика, подводное световое поле, уравнение переноса излучения, первичные гидрооптические характеристики, отношение сигнал/шум, дальность видимости в воде, наблюдение через взволнованную морскую поверхность.

L. S. Dolin[1], *I. M. Levin*[2]
[1]Institute of Applied Physics, N. Novgorod, Russia
[2]Saint-Petersburg Branch of the P. P. Shirshov Institute of Oceanology of RAS, Russia
Lev.Dolin@hydro.appl.sci-nnov.ru

THEORY OF UNDERWATER IMAGING

The paper presents an overview of the underwater imaging problem. A history of this problem is given. A universal underwater imaging theory is intended for computing image parameters and the maximal visibility distance of an extended target with inhomogeneous reflectance for various, including laser, underwater imaging systems. We consider the main elements of this theory: image transfer equation, beam spread function and modulation transfer function, the algorithms for computing image parameters of a target of limited size and the maximal visibility distance in water. Parameters of underwater light field, which are necessary for these algorithms, are given as a result of solution of the radiative transfer equation in terms of the water inherent optical properties. We present also a universal model of water inherent optical properties for wavelength close to 550 nm which makes it possible to determine all IOPs required for the underwater imaging theory using only the water attenuation coefficient or even Secchi depth. An algorithm for calculating the signal/noise ratio and the maximal sighting range in water are presented and used for comparison of efficiency of the imaging systems of various types. The main directions of the current investigations on the underwater imaging problem are considered, in particular, imaging through wavy sea surface.

Key words: underwater imaging, image transfer equation, beam spread function, modulation transfer function, underwater light field, radiative transfer equation, water inherent optical properties, signal/noise ratio, sighting range in water, imaging through wavy sea surface.

Humans in all times endeavored to look into sea depth as far as possible. However, the average sighting range in water is a thousand times shorter than in clear air. Submerged objects, and the sea bottom in coastal waters usually may be seen at depths no greater than several tens of meters. The hydrological optics as a science has its origin in the investigations of visibility of submerged objects. The underwater imaging problem occupies a particular place in the modern ocean optics: on the one hand, it comprises the theory of radiative transfer in water and, on the other hand, has the most distinct practical implementation. Indeed, optical imaging systems are of considerable current use for study and investigations of the World Ocean. They are applied to look for minerals and sunk objects at the sea floor, to map distributions of vegetation and bottom sediments, to detect bottom pollution, and to monitor regions of marketable fish spawning. Optical imagers can sense the effects of anthropogenic and natural processes including bottom changes, beach destruction, suspended matter in rivers and current flows. In all these applications the most important problem is an increase of the sighting range in water and improving the quality of underwater target images. Indeed, the more the sighting range, the more (for the same viewing angle) the productivity of the underwater survey (area observed increases with altitude squared), and the less expenditure of fuel and other resources.

It has been just a hunger for increase of a sighting range in water which had led to rapid progress of ocean optics in sixties-eighties due to financing the hydro-optical investigations by navy departments. At that time, after producing lasers working in the blue-green spectral range where oceanic water is most transparent, a lot of publications in USSR and USA promised tenfold and more increase of the sighting range in water. Once the Soviet cosmonauts had communicated that they saw the ocean floor at the depth of 6 km, some authors explained this effect by various fantastic causes, i. e. light focusing by sea surface waves, and then the claims to increase of underwater visibility further grew. In general, the problem of underwater imaging always was surrounded by various exotic inventions, false discoveries, spending a great amount of money on the undoubted deadlock researches. Meanwhile, the practical problem of improving underwater visibility may be apparently solved only on the basis of adequate imaging theory applicable to any optical imaging system. Such system comprises a light source, natural (the Sun and the sky) or artificial (in particular, a laser), and a receiver which consists of an objective lens and a photo-detector (the film, the photodiode, the photomultiplier, or the TV-tube), and is intended for observation of an arbitrary underwater object. The latter may be the sea floor and objects of any size and shape lying at it, or an isolated target (e. g., a Secchi disk) placed in the water body. The imaging system itself may be submerged — then we deal with a case of the purely underwater observation, or may be placed in air (at the ship, aircraft or satellite) — then the observation is performed through wavy sea surface.

The main reasons of the loss of visibility and the degradation of the image quality which should be taken into account in an imaging model are following:

1. Light scattering and absorption in water blurs imagery causing an information loss for the small details of observed objects. Thus the useful informational signal formed by light reflected from the object and reaching the receiver without scattering, is rapidly damped out with a distance between the target and the receiver, while the detrimental signal formed by the forward-scattered light, increases and leads to the image blurring.
2. Light backscattered by the water body and, in the case of observation from air, by sea surface and atmosphere, causes a veiling haze, which does not virtually depend on the presence of the target and shields the target, provoking a decrease of the image contrast. However, if to place the light source tightly to the target, or if to observe the self-luminous (lighted from behind) object, or to use the short pulses for illuminating the object, the veiling haze can be almost entirely eliminated.
3. Nevertheless, when the distance between the receiver and the target further increases, the self-luminous object also becomes invisible; it disappears on the background of a blur formed by small angle light scattering on the way from the target to the receiver. This image diffusion is quantitatively determined by Modulation Transfer Function (MTF) — we will consider it below.
4. When observing the sea floor from air, owing to light refraction on the randomly — inhomogeneous sea surface, the bottom image becomes randomly-inhomogeneous as well, while light reflected from the surface brings additional noises into the image.

The extent to which the image quality is affected by these factors depends on the observation conditions. These conditions include the nature of the viewed objects or the bottom area, the water inherent optical properties (IOPs), the state of the sea surface and atmosphere, the Sun position, and the imaging system itself. An underwater imaging theory aims to find the relations between the parameters of an imaging system, a viewed object (target), a light source, the seawater, the sea surface and the atmosphere. Overall, this theory is to recommend the optimal parameters of the imaging systems so that the sighting range in water and the image quality would be maximal.

Some history of the underwater imaging theory. For a long time the only means of underwater viewing were the human eye and the photo-camera. With regard to such viewing, Duntley and Preisendorfer had developed a visibility theory in a series of papers dated 1949–1957 which after that was included in a number of well-known monographs and overviews on hydrological optics (see, e. g. [1–5]). This «classic» theory of underwater visibility is intended to calculate the sighting range of a small uniform target against the water background under daylight. Later, the progress in development of the more sophisticated observation means and green lasers demanded a more universal imaging theory. The Universal Underwater Imaging Theory (UUIT) which involves the general case of imaging an extensive object with arbitrary spatial structure, includes the concepts of the Beam Spread Function (BSF) and MTF of water and deals with the cases of both natural and artificial (including laser) illumination, was originally developed and published in 1969 by Levin [6], and Bravo-Zhivotovsky, Dolin, Luchinin and Savel'ev [7]. These papers include also the theoretical and experimental data on propagation of a narrow light beam in water, in particular, BSF, needed for computing parameters of the image of an arbitrary object. In USA the similar theory was first published in 1977 by Mertens and Replogle [8]. Later this theory was presented in a number of papers. The most complete description of the universal theory of underwater imaging is presented in the monograph of Dolin and Levin [9] and in the overviews of the same authors [10, 11]. Theory of imaging through wavy sea surface is contained in the monograph of Dolin, Gilbert, Levin, and Luchinin [12]. Underwater imaging theory was studied also by E. Zege, A. Ivanov and I. Katzev (Belarus), G. Gilbert, J. Jaffe (USA) et al. Further we consider the main results of UUIT.

Classification of imaging systems. Let us consider the presently accepted classification of imaging systems (fig. 1). We distinguish them by the width of the directional diagrams of the light source (*SD*) and receiver (*RD*).

Note that the light source diagram $SD = D_s(\bullet)$ is dependence of the light source radiant intensity on the angle with beam axis; the receiver diagram $RD = D_r(\bullet)$ determines relative sensitivity of the photo-detector to the radiance entering the receiver at different angles to its axis. The width of *RD* is determined by the solid angle inside which the light flux, forming one image element, enters the receiver.

In the system *1*, a narrow light beam scans the target plane; the *RD* coincides with its viewing angle, while a receiver contains one-element photo-detector (e. g., a photomultiplier).

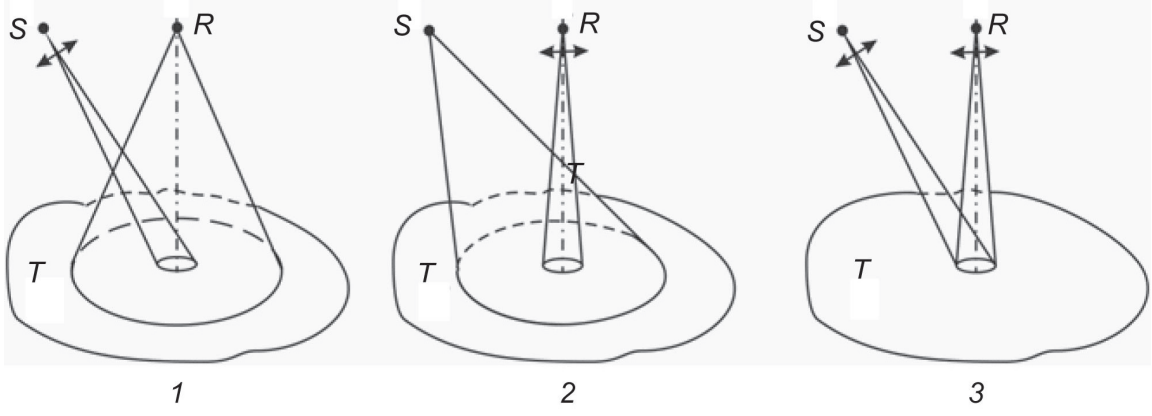

Fig. 1. Classification of imaging systems.
S is the light source, *R* is the receiver, *T* is the target plane.
1 — *SD* is narrow, *RD* is wide; *2* — *SD* is wide, *RD* is narrow; *3* — both *SD* and *RD* are narrow.

By the system *2* we mean a traditional TV- or photo-system with a multi-element photo-detector (an image tube, a film, or a CCD matrix). The target plane is illuminated uniformly by daylight or by an artificial light source with wide *SD*, the solid viewing angle of the receiver is *N* times greater than the solid angular width of the narrow one-element *RD*, where *N* is the total number of image elements in the image frame.

The system *3* as well as the system *1*, includes the narrow beam (narrow SD) and one-element detector (a photomultiplier), while its *RD* is narrow, as in the system *2*. The image in this system is formed as a result of synchronous scanning the target plane by both narrow diagrams, *SD* and *RD*.

Any one from the systems of three types may be continuous or pulsed. In the latter case the system works in gating regime, that is, to eliminate the veiling haze, the «closed» sensor is unlocked in the moment when the reflected from the target pulse comes to the sensor.

Image transfer equation. Point spread function and modulation transfer function. We define an image as distribution of the total radiant power P which enters the receiver and forms an image element as a function of the directions of the axes of the light source ($\vec{n}_s$) and receiver ($\vec{n}_s$), and the target reflectance distribution $R(\vec{r}_t)$:

$$P = P_t + P_w, \tag{1}$$

$$P_t(\vec{n}_s, \vec{n}_r, z) = \frac{P_0 \sum_r \Delta\Omega_r}{\pi} \iint_{\infty} R(\vec{r}_t) E_s(\vec{r}_t, \vec{r}_{0s}, z) E_r(\vec{r}_t, \vec{r}_{0r}, z) d\vec{r}_t \ , \tag{2}$$

where P_t is the signal due to light reflected from the target, P_w is the detrimental veiling light signal or haze due to backscattered light in the water not associated with the target, P_0 is the light source power, $\sum_r$ is the area of the objective entrance pupil, $\Delta\Omega_r$ is the solid angle determining the width of *RD*, $\vec{r}_{0s}$ and $\vec{r}_{0r}$ are the points of interaction of directions $\vec{n}_s$ and $\vec{n}_r$ with the target plane, z is the distance between the receiver and the target plane; E_s is the distribution of the irradiance on the bottom plane; the term E_r is a mathematical artifice representing the receiver directional diagram projected on the bottom. It is equivalent to the irradiance at the point on the bottom $\vec{r}_t$ which would have come from an auxiliary light source of unit power located at the receiver objective and having an angular radiant intensity distribution identical to the directional diagram of the receiver (fig. 2). Equation (2) is derived using the reciprocity theorem for a turbid medium. This theorem is valid for both optically homogeneous media and for media separated by a common boundary. This equation is conventionally referred to as the image transfer equation.

The functions E_s or E_r, as one can see from fig. 2, can be expressed as integrals over product of directional diagram *SD* or *RD* by the functions e_s or e_r which are the irradiance distributions in the target plane from unidirectional light beam with unit power, placed into the point *S* or *R* and emitting in direction $\vec{\Omega}$:

$$E_{s,r} = \frac{1}{\Delta\Omega_{s,r}} \iint_{(\vec{\Omega}\cdot\vec{n}_{s,r})>0} D_{s,r}(\vec{\Omega} \wedge \vec{n}_{s,r}) e_{s,r}(\vec{\Omega}, \vec{r}_t) d\Omega \ , \tag{3}$$

where $\Delta\Omega_s$ is the solid angle determining the width of *SD*, $D_s(\bullet)$ and $D_r(\bullet)$ are *SD* and *RD* respectively. The equations (1)–(3) are valid both for continuous and pulsed imaging systems. In the latter case by P_0 one should mean the average power of the pulsed light source. However, the detrimental signal P_w for a pulsed system differs greatly from P_w of a continuous system (see below).

The image transfer equation gives the entire information about image structure in an arbitrary imaging system. However, in practice, it is more convenient to use parameters which directly define the image quality. Such parameters are the point spread function (PSF) and MTF.

If the viewing angle is not very large, the isoplanatism hypothesis holds, that is, one can ignore the variation of the functions E_s or (and) E_r during scanning. Then we can replace the functions E_s and E_r by the irradiance distributions $E_{s\perp}$ and $E_{r\perp}$ from the real and auxiliary light sources of unit power. Accordingly, the functions e_s and e_r in eq. (3) can be replaced by the BSF which is an irradiance distribution from unidirectional light beam of unit power in the plane, normal to the beam axis (fig. 3).

Then we can rewrite eq. (2) in the form similar to the image of a traditional optical system, that is, in the form of a convolution of the target reflectance, R and a function Q, i. e.

$$P_t(\vec{r}_0, z) = P_0 \eta_\infty \iint_\infty R(\vec{r}_t) Q(\vec{r}_0 - \vec{r}_t, z) d\vec{r}_t \ , \tag{4}$$

where

$$\eta_\infty = \frac{\sum_r \Delta\Omega_r}{\pi} \iint_\infty E_{s\perp}(\vec{r}_\perp, z) E_{r\perp}(\vec{r}_\perp, z)\, d\vec{r}_\perp \ , \tag{5}$$

$$Q(\bullet) = \frac{E_{s\perp}(\vec{r}_\perp, z) E_{r\perp}(\vec{r}_\perp, z)}{\iint_\infty E_{s\perp}(\vec{r}_\perp, z) E_{r\perp}(\vec{r}_\perp, z) d\vec{r}_\perp} \ .$$

where $\Delta\Omega_r$ is the solid angle of RD, $\vec{r}_0$ is a point of interaction of the axis of the narrow diagram (SD in the system 1, RD in the system 2, SD and RD in the system 3) with the target plane, $\vec{r}_\perp$ is the radius-vector of a point, counted from beam axis (see fig. 3).

If to look attentively at eqs. (3)–(5), it is seen that the function η_∞ is the coefficient of light power transfer from a hypothetical infinite Lambertian plane of reflectance $R(\vec{r}_t) \equiv 1$ placed at the position of the

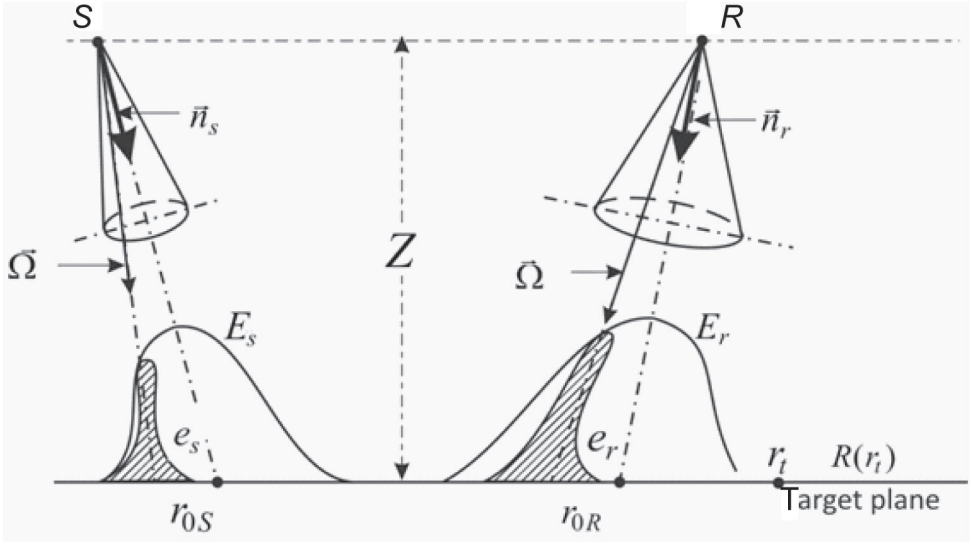

Fig. 2. Schematic diagram of the arbitrary imaging system.

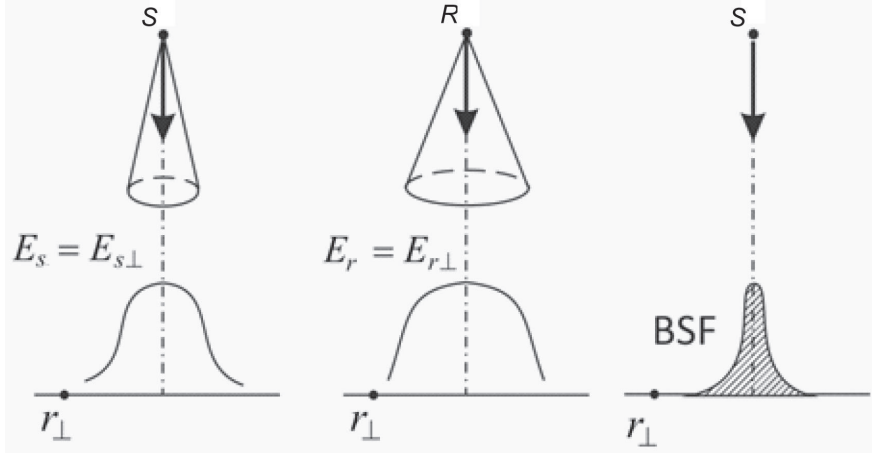

Fig. 3. Schematic diagram of functions E_s, E_r corresponding to isoplanatism hypothesis, and BSF.

real target plane (e. g. sea bottom), $Q(\vec{r}_\perp, z)$ is the Point Spread Function (PSF) of the imaging system, which defines the image of a point and implies the normalization conditions

$$\iint_{\infty} Q(\vec{r}_\perp, z)\, d\vec{r}_\perp = 1.$$

It defines the image structure for an underwater imaging system as does the PSF of traditional optical systems. However, unlike the PSF of the traditional optical systems, $Q(\vec{r}_\perp, z)$ depends on other factors affecting the image including the water medium.

In addition to the PSF, the MTF may be used to characterize the image of an underwater target. According to convolution theorem, it follows from eq. (4) that

$$\tilde{P}_t(\vec{\nu}, z) = P_0 \eta_\infty \tilde{R}(\vec{\nu}) \tilde{Q}(\vec{\nu}, z), \tag{6}$$

where the tilde indicates a two-dimensional Fourier transform of the function. Equation (6) shows that the imaging system in water acts as a linear filter of spatial frequencies $\vec{\nu}$. The gain-frequency characteristic of this filter $\tilde{Q}(\vec{\nu}, z)$ is referred to as the MTF.

Let us consider the image, $P_t(\vec{r}_0, z)$, of an infinite target with a sinusoidal distribution of reflectance

$$R(\vec{r}_t) = < R > [1 + C_0 \cos(\vec{\nu}\vec{r}_t)], \tag{7}$$

where <R> = 0.5(R_1+R_2) and R_1, R_2, and <R> are the maximum, minimum and average values of R. Then

$$C_0 = (R_1 - R_2)/(R_1 + R_2)$$

is the inherent contrast of R, and $\nu = 2\pi / l$, where l is the spatial period of the target's sinusoidal reflectance. If to substitute the distribution (7) in eq. (4), we obtain

$$P_t(\vec{r}_0, z) = < P_t > [1 + C_t \cos(\vec{\nu}\vec{r}_0)]$$

$$C_t = C_0 \mathrm{MTF} = (P_{t1} - P_{t2})/(P_{t1} + P_{t2}) \tag{8}$$

that is, C_t is the apparent contrast of the image (without haze); P_{t1} and P_{t2} are the maximum and minimum of $P_t(\vec{r}_0, z)$, and $<P_t> = <R>\ P_0 \eta_\infty$.

Equation (8) shows that MTF of an imaging system is the ratio of apparent and inherent contrast (in the absence of haze) as a function of the target spatial frequencies, ν_x, ν_y. This function defines the amplitude distortion of an image.

Thus, the sinusoidal structure **(**eq. (7)**)** is transferred in water without distortion with only amplitude changes. The MTF is the ratio of the apparent and inherent contrasts, i. e. the contrast of the image and the target, as a function of spatial frequency. Actually, the MTF carries no more information than the PSF, but facilitates the direct calculation of the image contrast of an infinite Lambertian target with a sinusoidal reflectance distribution.

Thus, the image of any underwater target can be calculated by using eqs. (1) and (4), when the values of η_∞, P_w, and the PSF or its spectrum, the MTF, are known. All of these functions may be expressed using parameters of underwater light fields from natural and artificial illumination.

Image parameters of a target of limited size. The MTF can be used for computing a contrast of an infinite target. However, the most typical problem of the underwater imaging theory is distinguishing small details on a target of limited size, generally treated as a disk with diameter d and periodic distribution of reflectance **(**eq. (7)**)**, placed on the some uniform background. In this case the total signal which is the radiant power P forming an image element, includes the signals from the target and background, and the detriment signal determined by light backscattering in water:

$$P(\vec{r}_0) = P_t + P_w + P_b. \tag{9}$$

It follows from eq. (4) that for this target the coefficients of light power transfer and the contrast (without haze)

$$\eta_t = P_t / P_0 = \langle R \rangle \eta_\infty F_\Sigma, \tag{10}$$

$$\eta_b = R_b \eta_\infty (1 - F_\Sigma), \tag{11}$$

are expressed through a parameter

$$C_t = \frac{\mathrm{MTF} \cdot C_0}{F_\Sigma}, \qquad (12)$$

$$F_\Sigma = \int_\Sigma Q(\vec{r}_\perp, Z) dr_\perp ,$$

which is the integral of the PSF over the target surface. Obviously, $F_\Sigma = 1$ for an infinitive target. For small targets $F_\Sigma << 1$, and it follows from eq. (12) that the smaller the object size Σ (and thus F_Σ) the greater the contrast of a target details. Misunderstanding this fact sometimes gave birth to publications about discovery of false effects of anomalous sighting range in water [13]. Note that for the systems 1 and 2 the parameter F_Σ coincides with a value of $P_\Sigma(z)/P_\infty(z)$ which is a ratio of the light power passing through a round cross-section Σ at the distance z from a unidirectional light source to the light power passing through the infinite cross section at the same distance.

Required parameters of light field in water. Considered results of the image transfer theory show that for calculating the image properties one should know, besides the imaging system parameters $\Omega_{s,r}$, *SD*, *RD*, P_0, Σ_r, a number of parameters of the light field in water for narrow and wide, continuous and pulsed light beams. There are the coefficient of light power transfer from a hypothetical infinite Lambertian plane of unit reflectance η_∞, PSF, MTF, and parameter F_Σ for the systems *1*, *2* and *3*. All numerated parameters are functions of BSF which is an irradiance distribution from unidirectional light beam of unit power in the plane, normal to the beam axis. Besides, in accordance with reciprocity theorem, the BSF coincides with the angular radiance distribution from a point light source, consequently, for the systems *1* and *2* PSF = BSF. Therefore, BSF may be considered as the main light field characteristic for underwater imaging problem because it can be used for calculation of all other required light field parameters. Nevertheless, it is convenient to have available simple equations or ready for use results of calculating the other light field parameters. Besides, it is necessary to know the haze power P_w for continuous and pulsed light sources, as well as some parameters of natural light field. The latter determine the useful image signal in the system *2* working under natural illumination, and the haze in the laser systems *1* and *3* working in the day-time. They are the vertical attenuation coefficient and remote sensed reflectance (RSR).

All numerated light field parameters are functions of the water IOPs: absorption (*a*), scattering (*b*), and backscattering (b_b) coefficients and phase function $\beta(\theta)$. They were computed by solving the radiative transfer equation (RTE) for turbid media:

$$\left(V^{-1} \frac{\partial}{\partial t} + \vec{\Omega} \nabla_{\vec{r}} + c \right) L(\vec{r}, \vec{\Omega}, t) = \frac{b}{4\pi} \int_{4\pi} L(\vec{r}, \vec{\Omega}', t) \beta(\theta) d\Omega'$$

where *L* is the radiance in the point $\vec{r}$ in the direction $\vec{\Omega}$ at time *t*, *V* is the light velocity, $c = a + b$ is the attenuation coefficient, and $\theta = (\vec{\Omega} \wedge \vec{\Omega}')$ is the scattering angle.

Accuracy of RTE solutions was corroborated by laboratory and field experiments and by Monte Carlo simulations. Let us consider these solutions.

The BSF, η_∞, MTF, and parameter F_Σ were computed in the small-angle approximation. The coefficient of light power transfer from a target for the systems *1* and *2* (a superscript in parenthesizes shows the system type):

$$\eta_\infty^{(1)} = \frac{\Sigma_r}{\pi z^2} \exp(-2a_1 z), \qquad \eta_\infty^{(2)} = \eta_\infty^{(1)} / N ,$$

where $a_1 = a + 2b_b$, *N* is the number of elements in the image frame. The systems *1* and *2* are supposed to be «reversible», that is, their narrow and wide diagrams are the same:

$$SD^{(1)} = RD^{(2)}, \; SD^{(2)} = RD^{(1)}. \qquad (13)$$

Integral of BSF over the target plane $P_\Sigma / P_\infty = F_\Sigma^{(1,2)}$ is expressed by equation

$$F_\Sigma^{(1,2)}(bz, q\theta_t) = (q\theta_t) \exp(-bz) \int_0^\infty (x + \sqrt{1 + x^2})^{bZ/x} J_1(q\theta_t x) x dx \cdot \qquad (14)$$

Here $2\theta_t$ is the angular size (d/z) of the round target, $J_1(...)$ the Bessel function, *q* is the parameter of the

forward part of the water phase function expressed by the function $\beta(\theta) = (1 - 2\tilde{b}_b)2q\theta^{-1}\exp(-q\theta) + 2\tilde{b}_b$, where $\tilde{b}_b = b_b / b$ is the backscattering probability. The paramrter q describes the anisotropy of the phase function and for various water turbidity ranges from 5 to 9. Accuracy of eq. (21) was confirmed by measurements and Monte Carlo computations.

The functions $F_\Sigma^{(1,2)}$ calculated by eq. (14) and numerically computed $F_\Sigma^{(3)}$ for different bz и $q\theta_t$ are given in fig. 4.

The BSF was numerically computing by differentiation of eq. (14). The MTF for the systems *1* and *2* is expressed by a simple equation:

$$\mathrm{MTF}(\psi, z) = \exp(-Abz) , \qquad A = 1 - (\psi^*)^{-1} \ln\left[\psi^* + \sqrt{1 + (\psi^*)^2}\right],$$

where $\Psi^* = 2\pi q\Psi$, $\Psi = z/(2l)$ is the angular spatial frequency, Z is the distance of observation, l is the size of resolved element in the target plane. Numerically computed MTF of the system *3* is much greater than $\mathrm{MTF}^{(1,2)}$.

The light power of a haze for the systems *1* and *2* with a continuous light source, if the condition (13) is valid,

$$P_w^{(1)} = \pi^{-1} P_0 \Sigma_r b_b [k^{-1}\exp(-a_1 k) + a_1 Ei(-a_1 k)], P_w^{(2)} = P_w^{(1)} / N ,$$

where $k = l_{sr}\tan^{-1}(0.5\vartheta)$, Ei is exponential integral function, l_{sr} is the distance between light source and receiver in the imaging system («base»), $a_1 = a + 2b_b$, 2ϑ is an angle defining the width of the diagram RD in the system *1* (field angle), Ei is the exponential integral.

For the pulsed systems:

$$P_w^{pulse(1)} = \frac{P_0^{pulse}\Sigma_r b_b V \Delta t}{4\pi z^2}\exp(-2az), \qquad P_w^{pulse(2)} = P_w^{pulse(1)} / N ,$$

where P_0^{pulse} is the initial power of the light pulse, V is the light speed in water, Δt is the initial pulse duration, P_w^{pulse} is the pulsed power of backscattered light in the moment of receiving the pulse reflected from a target. Here we again suppose that the condition (13) is valid.

For the imaging systems, working under natural illumination, eqs. (9), (12) are valid, while instead of eqs. (10), (11) the light power from a target and background are expressed as:

$$P_t = \frac{\Delta\Omega_r \Sigma_r}{\pi} E_d(z) < R > F_\Sigma \exp(-az) , \qquad (15)$$

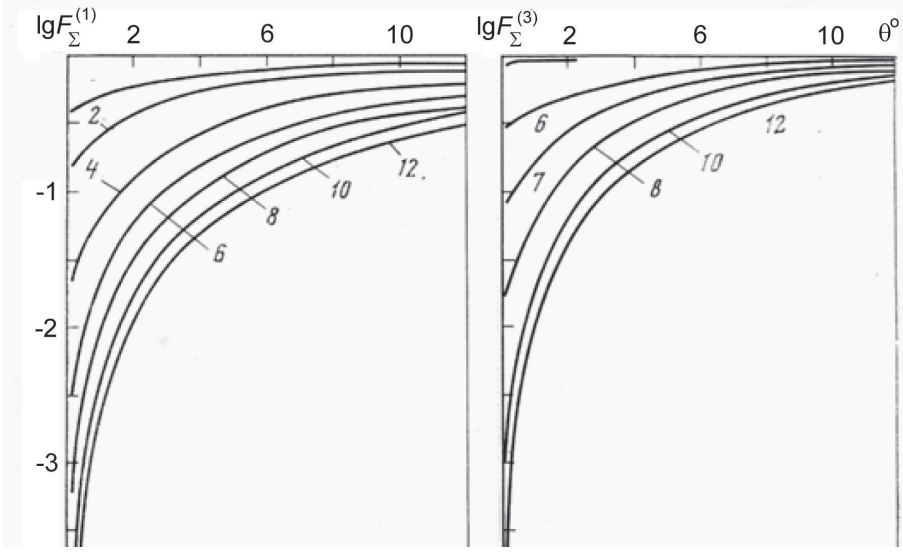

Fig. 4. The values of parameters $F_\Sigma^{(1,2)}$ and $F_\Sigma^{(3)}$ as functions of angular size $2\theta = 2\theta_t$ of the section Σ for typical for seawater value of $q = 7$.
The numbers of curves are the optical distances bz.

$$P_b = \frac{\Delta\Omega_r \Sigma_r}{\pi} E_d(z) < R_b > (1 - F_\Sigma) \exp(-az) \ ,$$

where $E_d(z)$ is irradiance at the depth z of the viewed target.

Attenuation of underwater irradiance with depth is expressed as

$$E_d(z) / E_d(0) = \exp(-K_d z) \ , \tag{16}$$

where $K_d(z)$ is the vertical attenuation coefficient which is slightly greater than absorption coefficient a, but less than attenuation coefficient c.

The most simple and rather accurate expression for K_d is the solution of RTE in quasi-single scattering approximation (QSA) [9]:

$$K_d = D_d(a + b_b) \ . \tag{17}$$

For direct solar irradiance the coefficient $D_d \cong 1.04 / \cos\theta_0'$, where θ_0' is the refraction angle ($\sin\theta_0' = \sin\theta_0 / n$, θ_0 is the solar zenith, n the water refractive index). For diffuse illumination from the sky $D_d \approx 1.16$.

Monte Carlo simulation [9] showed that accuracy of QSA is rather high up to optical depth $\tau = cz = 5–7$, while for greater τ it decreases. Nevertheless, the simple QSA eq. (17) is widely used, especially for calculation in subsurface sea layer.

The most accurate (but more cumbersome than QSA) solution of RTE for downwelling underwater irradiance which is valid for any depth, was obtained in the self-similar approximation. It is given in the monographs [9, 12] and in encyclopedias [10, 11].

The light power of haze for natural illumination is expressed as

$$P_w = \pi^{-1} \Sigma_r \Delta\Omega_r E_d(z_s) \rho \ ,$$

where $E_d(z_s)$ is irradiance at the depth $z = z_s$ of an imaging system, $\rho = \pi L_u(z_s) / E_d(z_s)$ is the Remote Sensing Reflectance (RSR), in Russian literature referred to as radiance coefficient, L_u is upwelling radiance in the point of observation z_s. Monte Carlo computations showed that RSR can be calculated with rather high accuracy in QSA:

$$\rho = A_\rho b_b / (a + b_b) \ ,$$

The coefficient A_ρ depends on the observation direction, solar zenith angle, and a fraction of the molecular scattering in the backscattering coefficient b_b. However [12], an average value of $A_\rho = 0.275$ with dispersion ±5 % is valid for any illumination conditions. Another authors have found rather close values of A_ρ: 0.298 [14], 0.295 [15].

The signal/noise ratio, sighting range and spatial resolution in water. The image transfer theory, together with parameters of the light field of narrow and wide light beams make it possible to solve the first part of the underwater imaging theory: computation of «regular» image parameters, determined by light absorption and scattering in water. However, beside the regular component, an image always includes noises. Just the noises determine the sighting range and spatial resolution in water.

For underwater imaging systems, sighting range is determined mainly by internal photon (shot) noise. The value of signal/noise ratio (SNR) due to shot noise is

$$\Psi = C\sqrt{n_e} = C\sqrt{Q / e} = C\sqrt{\eta_d PT / e} \ , \tag{18}$$

where C is the image contrast with regard to all components of the signal (due to the target, haze and background); n_e is the average number of electrons, Q the average charge, and P the total average signal power at an image element formed by light reflected from the target and background (sea bottom or water body), and light backscattered in water; η_d is the spectral sensitivity of the detector photocathode; T the duration of charge accumulation at the image element; $e = 1.6\ 10^{-19}$ coulombs is the elementary charge. SNR Ψ is a function of the distance z between the target and the imaging system and of the spatial frequency ν. To find the sighting range $z_{max}(\nu)$ or the spatial resolution $\nu_{max}(z)$ one should solve the equation $\Psi(z, \nu) = \Psi^*$ with respect to z or ν, where Ψ^* is the threshold (usually equals 2–5) of SNR.

The model of IOPs for wavelength about 550 nm. To use the underwater imaging theory in practice it is convenient to have a few-parameter optical model of seawater IOPs. The image quality and the sighting range in water depend on IOPs: absorption (a), scattering (b), backscattering (b_b) coefficients and the phase function parameter q. However, the measured data on these IOPs are poorly known. Most of all data is available on the measured attenuation coefficient $c = a + b$. The single thoroughly studied water parameter is the Secchi depth z_d: detailed maps exist of z_d distributions for the World's Ocean [16, 17]. We have found the relations between IOP which permits to calculate a, b, b_b, and q in the spectral range 500–550 nm (as a rule, most of underwater imaging systems work in this spectral range) using the measured value of the attenuation coefficient $c = a + b$ in the same spectral range.

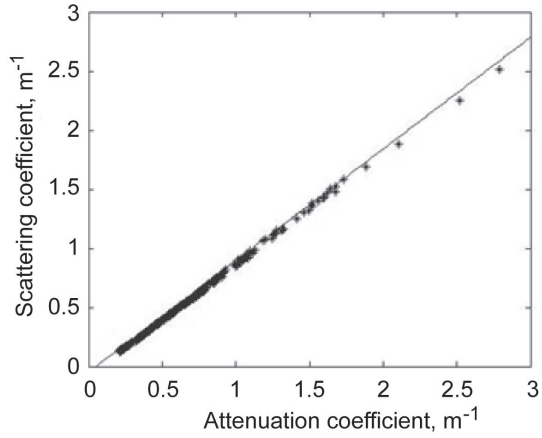

Fig. 5. Relations between the scattering coefficient and the attenuation coefficient at 550 nm.
The dots show the data sampled in the Baltic Sea at 555 nm, and the line represents eq. (19) obtained for ocean waters at 550 nm.

On the basis of some 70 measurements in the Atlantic and Pacific Oceans and in the Arabian Sea, Levin and Kopelevich [18] founded that c at wavelengths close to $\lambda = 550$ nm the linear relation between b and c:

$$b = 0.944c - 0.048 \tag{19}$$

with the standard deviation $\sigma_b = 0.033\ m^{-1}$.

Measurements in the Baltic Sea [19] show that despite the different sea regions and the different experimental procedure and instrumentation used, the relations between b and c in Baltic and ocean waters resemble each other very closely (fig. 5). Consequently, it can be concluded that the strong linear dependency between b and c at wavelength close to 550 nm is rather universal. In particular, given in [18] comparison of eq. (19) with data of b and c measured by Morel and Prieur [20] and Schoonmaker et. al. [21] in coastal and ocean waters shows rather good agreement between eq. (19) and these data.

On the basis of the established linear relation between c and b, the relationships between the attenuation coefficient c, the absorption a and backscattering coefficient b_b, and phase function parameter q at wavelength about 550 nm for Case 1 and Case 2 waters were obtained:

$$a = c - b = 0.056c + 0.048, \tag{20}$$

$$b_b = 0.018c, \tag{21}$$

$$b_b = 0/0183c - 0.0094b, \tag{22}$$

$$q = [2/(0.021 + 0.765b_b/b)]^{1/2}. \tag{23}$$

Equation (21) relates to the coastal water (Case 2), (22) to the ocean waters (Case 1); eqs. (20) and (23) are valid for both water types.

Besides, we have developed a model which relates c (550 nm) to the Secchi depth z_d [22, 23]. This model and eqs. (19)–(23) allow to find all necessary IOPs in the spectral range 500–550 nm by use of maps of Secchi depth z_d.

Comparison of efficiency of the imaging systems of various types. Underwater imaging theory provides a way to compare the capabilities of various imaging systems. In so doing, one should take into account the relationships between parameters of the systems *1*, *2* and *3*:

$$\mathrm{MTF}^{(1)}(\nu) = \mathrm{MTF}^{(2)}(\nu), \quad F_\Sigma^{(1)} = F_\Sigma^{(2)}, \; P^{(1)} = NP^{(2)}, \tag{24}$$

$$\mathrm{MTF}^{(3)} >> \mathrm{MTF}^{(1)}, \; P^{(3)} << P^{(1)}.$$

The relations (24) follow from the optical reciprocity theorem and condition (13) of «reversibility» of the systems *1* and *2*. For the systems *1* and *2*

$$T^{(1)} = T_f/N, \; T^{(2)} = T_f,$$

where T_f is the frame duration, N the number of elements in the image frame.

Note that all signal components are proportional to the area of the entrance pupil Σ_r, frame period T_f, and the initial power of the light source P_0. Then it follows from eqs. (18), (24), and (12) that for the systems with the similar light source (continuous or pulsed)

$$\frac{\Psi^{(1)}}{\Psi^{(2)}} = \sqrt{\frac{\Sigma_r^{(1)} T_f^{(1)} P_0^{(1)}}{\Sigma_r^{(2)} T_f^{(2)} P_0^{(2)}}} ,$$

while for continuous and pulsed systems of the same type (*1*, *2* or *3*) under condition that in the pulsed systems the backscattered haze is completely gated out

$$\frac{\Psi^{pulse}}{\Psi} = \sqrt{1 + \frac{P_w}{P_t + P_b}} . \qquad (25)$$

What can we conclude from these formulae?

If to compare the TV-system *2* with a laser scanner system *1*, we see that these systems ensure the same SNR and thus the same sighting range of the target with the same spatial frequency of its elements if these systems have the same regimes (continuous or pulsed), objective aperture, frame period and initial light source power. In the TV-systems the aperture is limited by a size of a detector (an image tube), usually not exceeded 40 mm, and the frame period 0.04 s. In the laser scanner system the aperture can be of any size, for example, by use of an array of detectors like photo-diode or multiplier, while the frame period is limited only by the speed of an underwater vehicle of the system and may be about 5–10 s. Thus, advantage of the laser system *1* is due to possible greater aperture and frame period. The system *3* ensures greater contrast, but lesser coefficient of light power transfer than system *1*, therefore it may be more effective only for the case of large power of the light source.

The pulsed system has advantage over the continuous system of the same type **(**as one can see from eq. (25)**)** when a small object is placed in the water body, and $P_w >> P_t$, $P_b = 0$. However, if we look at the sea bottom (especially the light one), the signal from the bottom is comparable and sometimes even greater than backscattered haze P_w, thus cutting the haze in the pulsed system do not ensure greater sighting range. We computed the sighting range of the TV-system of type *2* and the laser scanner continuous and pulsed systems of type *1* with parameters which values are currently achieved. The computations showed that the laser continuous system *1* ensures the sighting range 1.5 times greater than the TV-system *2* due to greater aperture (150 against 12 mm) and frame period (4 against 0.04 s), in spite of 5 times lesser power of the light source. The pulsed system *1* ensures enlargement of the sighting range of the Secchi disk (up to twice as compared with the continuous system *1*) due to gating of haze. However, the sighting range of both compared systems becomes almost the same, if to look at the sea bottom.

The sighting range of the bottom fragments (the average bottom reflectance $\langle R \rangle = 0.1$) by the pulsed system *1* as a function of the angular spatial frequency ψ of these fragments is shown in fig. 6 for different Secchi depths. The calculations were performed for the average bottom reflection $\langle R \rangle = 0.1$, the initial average power of the light source $P_0 = 1$ W, the aperture $d = 0.1$ m, the duration of image frame $T_f = 4$ s, the sensitivity of the photocathode $\eta_d = 0.04$ A/W, $N = 600 \times 600$, and $\Psi^* = 5$. Fig. 7 illustrates the sighting range of the targets of diameter 0.5 and 5 m (size of an element is 0.1 and 1 m, $\langle R \rangle = 0.1$) against background of water by pulsed system *1* with the same parameters as in fig. 6, as a function of the attenuation coefficient c and Secchi depth z_d.

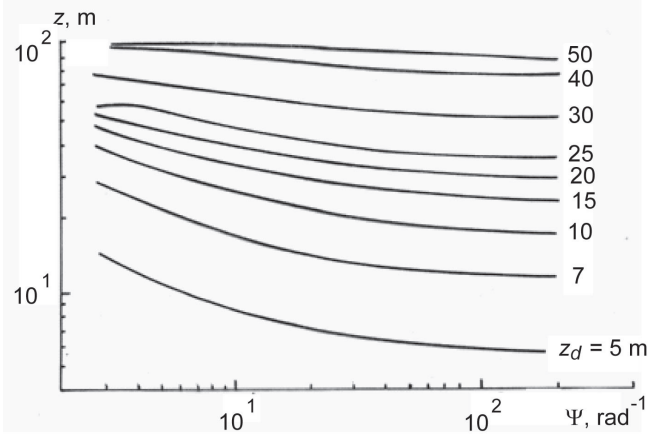

Fig. 6. Sighting range of bottom fragments for pulsed system *1* as a function of the angular spatial frequency for different Secchi depths z_d.

One can see from fig. 6 that the maximal sighting range of the large-scale fragments equals 100 m for Secchi depth $z_d = 50$ m. The sighting range stops to change when the angular spatial frequency achieves 100 elements/radian. However, if ψ > 1000 el/rad, the image will be fuzzy even

in very pure water at small distance due to turbulent fluctuations of the water refractive index. As seems, ψ = 100 el/rad may be considered as the maximal resolution in water. Fig. 7 shows that maximal visibility distance of the target of 5 m diameter ranges from 75 m in ocean waters (z_d = 50 m) to 20 m in coastal waters (z_d = 6 m). The sighting range of the target with 0.5 m diameter ranges from 65 to 12 m accordingly (if both targets have the same number (5) of resolved elements.

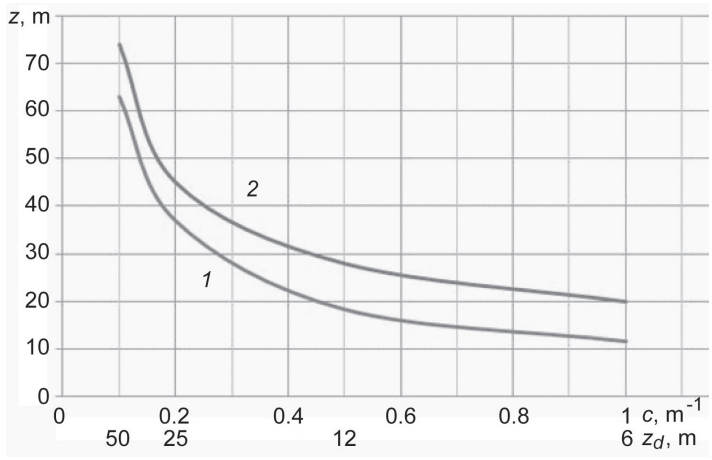

Fig. 7. Sighting range of a target of diameter 0.5 m (*1*) and 5 m (*2*), size of an element is 0.1 and 1 m, against background of water by pulsed system *1* as a function of the attenuation coefficient c and Secchi depth z_d.

Up-to-date problems of imaging in water. Let us consider the most up-to-date problems of imaging in water and the main directions of current investigations.

Improvement of the laser systems is directed to enlargement of the laser power, development of the new photo-detectors and the image processing facilities, as well as to development of compact laser systems with a very short pulse which can operate at night in very turbid water. Since the attenuation of irradiance in water with depth is exponential, it is important to choose the wavelength of laser radiation equal to the wavelength of minimal attenuation coefficient. Therefore, lasers with rebuilt frequency have big prospects. In general, the underwater laser systems are indispensable for working at large depth, for observation of the fine target fragments, for operating in turbid port waters.

Much attention is drawn to develop of lidars, which are the specific cases of the imaging systems. Lidars work on ships, aircrafts, and satellites. They are applied for study of sea waves and oil pollutions, for mapping the sea floor, for tomography of water, for detecting internal waves, for remote determination of organic matters through their luminescence. In particular, the inverse problems of retrieval of water IOPs from lidar signal were considered, and by use of measured in the Barents, White and Kara Seas correlations between IOP and hydro-physical properties, possibility of observation of internal waves (IW) and method of simulation of lidar images of IW were developed [24–26], and the process of passing the lidar signal through wavy sea surface was analyzed [27]. These investigations are explored further.

The one of advancement of underwater imaging theory is its extension to the systems with arbitrary field angle, since though the general equations of this theory are valid for any imaging system, the most important for practical purpose case eqs. (10)–(12) given above are true only for the systems *1* and *2* with wide field angle [28]. Besides, some authors proposed to use the modulated illuminating beam for enhancement of visibility distance in water [29–31].

One further direction is the observation of the sea shelf from a satellite under natural illumination, in particular, through thin clouds. Such observation is more effective for large-size objects or bottom fragments. As discussed above, currently more attention is focused on the problem of anomalous visibility of sea floor from space, communicated by cosmonauts. Of course, they cannot see the ocean floor at the depth of 6 km; however, an effect of increasing the sighting range with increasing the observer's height over the sea surface exists. The main reason of this effect is following. MTF for fixed size of the target element do not depend on height H, while MTF(ν)→1 if the spatial frequency ν→0. Therefore, illusory increase of sighting range with H may be explained by the fact that with increase of H an observer begins to see the large-scale bottom fragments which did not go into his viewing field from small H. The really maximal sighting range of the sea floor from space may be determined from eqs. (12), (15), (16) if to set C_0 = 1, MTF = 1, P_b = 0, F_Σ = 1, to add the radiance coefficients of pure atmosphere and sea surface to the radiance coefficient (RSR) of pure water, to replace the contrast C by the contrast threshold of the human eye C^* = 1 %, and to solve the obtained equation with respect to z for average reflectance $\langle R \rangle$ = 0.3

(a relatively light bottom) and minimal absorption coefficient $a = 0.005$ m^{-1} (wavelength $\lambda = 470$ nm). The solution is: $z_{max} = 520$ m.

Estimate of the prospect of imaging through clouds showed that it is possible to observe in shallow and pure waters the large scale light patches at the bottom under natural illumination through the thin clouds up to cloud optical thickness $\tau = 10$. The large-scale targets may be seen through more thick clouds (up to $\tau = 20–30$) as well, if to apply the pulsed imaging systems. Estimate of this possibility was made on the basis of the developed theory of pulse propagation in three-layer medium (cloud-atmosphere-water) which allows computing the energy, time delay and broading of a light pulse.

Currently much attention is given to the problem of applying the imaging systems for detection of the oil pollutions of the sea surface and water body both in the form of large patches and of the oil leakages from underwater pipeline wormholes, including the case of the water surface covered by ice [32–34]. These investigations are explored further.

Finally, currently the wide investigations are carried out on the problem of imaging through wavy sea surface. Note that airborne observation of the sea shelf and of objects laying on the sea bottom or submerged in the water is a much more efficient way to survey an area than are shipborne methods. For the same viewing angle the bottom area at a depth z when viewed from an altitude H over the sea surface is about $(H/z)^2$ times greater than when viewed from a point on the sea surface. Since the altitude H is usually much greater than the bottom depth, and the speed of a survey airplane is much greater than that of a ship or underwater vehicle, the gain in the survey productivity as well as savings in fuel and other resources is considerable. However, a major disadvantage of airborne imaging is due to the negative influence of surface waves on image quality. Surface waves introduce additional noise due to fluctuations of radiation seen by an imaging system. Such fluctuations are produced by the action of surface waves on the upwelling light reflected from the bottom, backscattered in the water body, and reflected from the surface. Besides, the sea surface waves produce strong distortions in the image. Light reflected from a submerged object is distorted by refraction through the random slopes of the rippled sea surface. The structure of these images may differ significantly from the structure of the imaged object because of random light refraction. The image may become broken and straight lines may convert into curves. The theory of imaging through wavy sea surface is given in the monograph [12]. Currently the main attention is given to the problem of correction of distorted by waves images. The first publications on this problem see, for example, in [35–37]. Currently the theoretical and experimental investigations of methods of correcting distorted by waves images with the aim of finding the methods, optimal for conditions of the real sea waves, are conducted in the Institute of Applied Physics, (N. Novgorod) and in the P. P. Shirshov Institute of Oceanology, St.-Petersburg Branch. One more new direction is determining the wind wave parameters necessary for the theory of imaging through sea surface, by underwater imaging systems located at the sea bottom [38].

Further development of the underwater imaging theory will go on the way of creation of the essentially new methods of underwater imaging: application of modulated and compound-modulated light beams for target illuminations, development of the systems forming volume images and the systems of automatic detection and identification of the underwater targets.

Acknowledgements. We thank our colleagues Natalia Pokrowskaya and Tamara Radomyslskaya for valuable help in preparing this paper.

The work was supported by the Russian Foundation for Basic Research under grants No 13-05-00050 and 15-45-02610.

References

1. *Duntley S. Q.* Light in the sea. *J. Opt. Soc. Am.* 1963. V. 53. P. 214—233.
2. *Preizendorfer R.* Hydrologic Optics. *Honolulu: NOAA*, 1976. 1750 p.
3. *Ivanoff A.* Introduction a L'oceanographie. *Paris: Librairie Vuibert*, 1975. V. 2. 392 p.
4. *Jerlov N.* Marine Optics. *New York: Elsevier*, 1976. 247 p.
5. *Ivanov A. P.* Phyzical background of hydrooptics. *Minsk: Nauka i technika*, 503 p. (in Russian).
6. *Levin I. M.* Observation of objects illuminated by a narrow light beam in a scattering medium. *Izv. Atmos. Ocean. Phys*. 1969. V. 5, N 1. P. 32—39.
7. *Bravo-Zhivotovsky D. M., Dolin L. S., Luchinin A. G., Savel'ev V. A.* Some problems of the theory of visibility in turbid media. *Izv. Atmos. Ocean. Phys*. 1969. V. 5, N 7. P.388—393.
8. *Mertence L., Replogle F.* Use of point spread and beam spread functions for analysis of imaging systems in water. *J. Opt. Soc. Am.* 1977. V. 67, N 8. P. 1105—1117.
9. *Dolin L. S., Levin I. M.* Handbook of the theory of Underwater Vision. *Leningrad: Gidrometeoizdat*, 1991. 230 p. (in Russian).

10. *Dolin L. S., Levin I. M.* Optics, underwater. *Encyclopedia of Applied Physics*. New York: VCH Publ. 1995. V. 12. P. 571—601.
11. *Dolin L. S., Levin I. M.* Underwater optics. Th. G. Brown et al. (Eds.): *The Optics Encyclopedia, Weinheim, Wiley-VCH Publ,* 2004. V. 5. P. 3237—3271.
12. *Dolin L. S., Gilbert G. D., Levin I. M., Luchinin A. G.* Theory of imaging through wavy sea surface. *N. Novgorod: Institute of Applied Physics*, 2006. 180 p.
13. *Duntley S. Q.* Underwater visibility and photography. *Optical aspects of oceanography. London—New York*: 1974. P. 135—149.
14. *Gordon H., Brown O., Evans R., Brown J., Smith R., Baker K., Clark D.* A semianalytic radiance model of ocean color. *J. Geophyz. Research*. 1988. V. 93, D 9. P. 10,909—10,924.
15. *Sydor M., Arnone R.* Effect of suspended particulate and dissolved organic matter on remote sensing of coastal and riverine waters. *Applied Optics*. 1997. V. 36, N 27. P. 6905—6912.
16. *Voitov V. I.* Secchi depth. Ocean optics. A. Monin [ed.], *Moscow: Nauka Publ.*, 1983. V. 2. P. 21—25 (in Russian).
17. Arnone R., Tucker S., Hilder F. Secchi depth atlas of the world coastlines. *SPIE Proceedings, 489, Ocean Optics VII*. 1984. P. 195—201.
18. *Levin I. M., Kopelevich O. V.* Correlations between the Inherent Hydrooptical Characteristics in the spectral range close to 550 nm. *Oceanology*. 2007. V. 47, N 3. P. 344—348.
19. *Levin I., Darecki M., Sagan S., Radomyslskaya T.* Relationships between inherent optical properties in the Baltic Sea for application to the underwater imaging problem. *Oceanologia.* 2013. N 55(1). P. 11—26.
20. *Morel A., Prieur L.* Analysis of variations in ocean color. *Limnol. Oceanogr.* 1977. V. 22, N 4. P. 709—722.
21. *Schoonmaker J. S., Hammond R. R., Heath A. L., Cleveland J. S.* A numerical model for prediction of sublittoral optical visibility. *SPIE Proc. Ocean Optics XII. Bergen: Society of Photo-Optical Instrumentation Engineers*. 1994. V. 2258. P. 685—702.
22. *Levin I. M., Radomyslskaya T. M.* Secchi disk theory: a reexamination // Current Research on Remote Sensing, laser Probing, and Imagery in Natural Waters, edited by I. M. Levin, G. D. Gilbert, V. I. Haltrin, and C. Trees. *Proceeding of SPIE*. V. 6615. 2007. 66150O (11 p.).
23. *Levin I. M., Radomyslskaya T. M.* Estimate of water inherent optical properties from Secchi depth. *Izv. Atm. Physics*. 2012. V. 48, N 2. P. 214—221.
24. *Dolina I. S., Dolin L. S., Levin I. M., Rodionov A. A., Savel'ev V. A.* Inverse problems of lidar sensing of the ocean // Current Research on Remote Sensing, laser Probing, and Imagery in Natural Waters, edited by I. M. Levin, G. D. Gilbert, V. I. Haltrin, and C. Trees. *Proceeding of SPIE*. 2007. V. 6615. 66150C (10 p.).
25. *Rodionov M. A., Dolina I. S., Levin I. M.* Correlations between depth distributions of water attenuation coefficient and density in north seas // *Fundam. prikl. gidrofiz*. 2012. V. 5, N 4. P. 39—46. (in Russian)
26. *Dolina I. S., Dolin L.S.* The effect of shear flow on the structure of lidar images of nonlinear internal waves // *Proceedings of the VII International Conference «Current Problems in Optics of Natural Waters» (ONW 2013). St.-Petersburg*. 2013. P. 12—15.
27. *Luchinin A. G.* Light pulse propagation along the path: atmosphere–rough surface–sea water // *Applied Optics*. 2010. V. 49, N 28. P. 5059—5066.
28. *Dolin L. S., Levin I. M.* Two approaches to computing the distance of underwater visibility // *Proceedings of the VII International Conference «Current Problems in Optics of Natural Waters» (ONW 2013). St.-Petersburg,* 2013. P. 124—127.
29. *Luchinin A. G.* Theory of an underwater lidar with a complex modulated illuminating beam // *Izv. Atmos. Ocean. Phys*. 2012. V. 48, N 6. P. 739—748.
30. *Luchinin A. G., Dolin L. S.* Complex modulated waves of photon density in underwater imaging // *Proceedings of the VII International Conference «Current Problems in Optics of Natural Waters» (ONW 2013). St.-Petersburg*, 2013. P. 24—27.
31. *Katsev I. L., Zege E. P., Prikhach A. S., Cochenour B., Mullen L.* Propagation of the modulated laser beam through sea water: comparison theory with experiment // *Proceedings of the VII International Conference «Current Problems in Optics of Natural Waters» (ONW 2013). St.-Petersburg,* 2013. P. 128—132.
32. *Levin I. M., Radomyslskaya T. M., Savchenko V. V.* Visibility of oil films on the water surface from space // *Fundam. prikl. gidrofiz*. 2012. V. 5, N 3. P. 75—84.
33. *Levin I. M., Radomyslskaya T. M.* et al. Possibility of oil film detection on the ice cover of the sea surface // *Proceedings of the Thirty-second Arctic and Marine Oil Spill Program (AMOP) Technical on Environmental Contamination and Response. Edmonton, Alberta. Canada. June 9—11*. 2009. V. 2. P. 781—789.
34. *Radomyslskaya T. M.* Oil film detection on the ice cover of the sea surface // *VII International Conference «Current Problems in Optics of Natural Waters» (ONW 2013). St.-Petersburg*. 2013. P. 195—198.
35. *Dolin L. S., Luchinin A. G., Titov V. I., Turlaev D. G.* Correcting images of underwater objects distorted by sea surface roughness. *Current Research on Remote Sensing, Laser Probing, and Imagery in Natural Waters. Proc. SPIE.* 2007. V. 6615, 66150K. 12 p.
36. *Turlaev D. G., Dolin L. S.* On imaging of underwater objects though a rough water surface: a new algorithm of image correction and a laboratory experiment // *Izv. Atmos. Ocean. Phys*. 2013. V. 49, N 3. P. 370—376.
37. *Levin I., Savchenko V., Osadchy V.* Correction of an image distorted by a wavy water surface: laboratory experiment // *Applied Optics*. 2008. V. 47, N 35. P. 6650—6655.
38. *Molkov A. A., Dolin L. S.* Determining the wind wave parameters by an underwater image of the sea surface // *Izv. Atmos. Ocean. Phys*. 2012. V. 48, N 5. P. 617—630.

Статья поступила в редакцию 14.07.2014 г.